174
12/24/80

(2)

Dr. 2155

R-880

MASTER ORNL/TM-7508

ornl

OAK RIDGE NATIONAL LABORATORY

UNION CARBIDE

Destabilization of Low Mode Number Alfvén Modes in a Tokamak by Energetic or Alpha Particles

K. T. Tsang
D. J. Sigmar
J. C. Whitson

OPERATED BY
UNION CARBIDE CORPORATION
FOR THE UNITED STATES
DEPARTMENT OF ENERGY

ORNL/TM-7508
Dist. Category UC-20 g

Contract No. W-7405-eng-26

FUSION ENERGY DIVISION

DESTABILIZATION OF LOW MODE NUMBER ALFVÉN MODES IN A TOKAMAK BY ENERGETIC OR ALPHA PARTICLES

K. T. Tsang, D. J. Sigmar, and J. C. Whitson

Date Published - December 1980

Prepared by the
OAK RIDGE NATIONAL LABORATORY
Oak Ridge, Tennessee 37830
operated by
UNION CARBIDE CORPORATION
for the
DEPARTMENT OF ENERGY

CONTENTS

ABSTRACT

With the inclusion of finite Larmor radius effects in the shear Alfvén eigenmode equation, the continuous Alfvén spectrum, which has been extensively discussed in ideal magnetohydrodynamics, is removed. Neutrally stable, discrete radial eigenmodes appear in the absence of sources of free energy and dissipation. Alpha (or energetic) particle toroidal drifts destabilize these modes, provided the particles are faster than the Alfvén speed. Although the electron Landau resonance contributes to damping, a stability study of the parametric variation of the energy and the density scale length of the energetic particles shows that modes with low radial mode numbers remain unstable in most cases. Since the alpha particles are concentrated in the center of the plasma, this drift-type instability suggests anomalous helium ash diffusion. Indeed, it is shown that stochasticity of alpha orbits due to the overlapping of radially neighboring Alfvén resonances is induced at low amplitudes, $e_i\tilde{\phi}/T_i \gtrsim 0.05$, implying a diffusion coefficient $D_r^\alpha \gtrsim 4.4 \times 10^3$ cm^2/s.

I. INTRODUCTION

In ideal magnetohydrodynamics, the shear Alfvén wave in a nonuniform medium satisfies a second-order differential equation that admits only a continuous spectrum. With the inclusion of finite Larmor radius effects, the second-order differential equation is replaced by a fourth-order one.[1,2] Discrete eigensolutions are possible because the Alfvén singularity is removed from the highest derivative. Rosenbluth and Rutherford first included this fourth-order finite Larmor radius term to investigate the excitation of shear Alfvén eigenmodes by energetic ions in a tokamak. (Earlier, Mikhailovskii had investigated this problem in the local approximation.[3]) However, in slab geometry the fourth-order term they derived is valid only for rather short radial wavelengths. In cylindrical geometry (or a torus with a very large aspect ratio), their fourth-order slab term is incompatible with the boundary condition at $r = 0$, where r is the minor radius. Therefore if one uses the Rosenbluth-Rutherford equation in cylindrical geometry, a global *unstable* mode can be found even when the energetic ion contribution is turned off; this is clearly a spurious result.

In Sec. II we present a derivation of the correct fourth-order eigenmode equation in cylindrical geometry. Using this equation, a quadratic form can be constructed to show that the eigenmodes are always neutrally stable in the absence of free energy and dissipation. Because of their large toroidal drift motion, the effect of alpha particles manifests itself predominantly through the current. The electrons contribute a stabilizing Landau resonance through the charge-neutrality condition. In Sec. III, the fourth-order radial eigenmode equation is solved numerically for several sets of (m,ℓ), the poloidal and toroidal mode numbers, and for all unstable radial modes characterized by n, the number of nodes of the eigenfunction. Section IV contains a discussion of an approximate local dispersion relation for both branches, $\omega = \pm k_{\parallel} V_A$, plus kinetic corrections, shedding some light on the parameter dependence of the instability. In Sec. V we use the numerical results of Sec. III to investigate the radial spacing of neighboring resonances and to estimate the magnitude of the fluctuation amplitude necessary for island overlapping of the perturbed alpha orbits, and, from that, we estimate the radial alpha particle diffusion coefficient in the stochastic state.

II. BASIC EQUATIONS AND THE QUADRATIC FORM

By averaging the gyrophase angle in the Vlasov equation, we obtain the perturbed densities for ion, electron, and alpha particles. Imposing the neutrality condition and ignoring the contribution of alpha particles because $N_\alpha \ll N_e$, N_i and $T_\alpha \gg T_e$, T_i, we have

$$\left(1 - \frac{\omega_{*e}}{\omega}\right)\left(\phi - \frac{\omega A_{\parallel}}{k_{\parallel} c}\right)[1 + \zeta_e Z(\zeta_e)] = \left(1 - \frac{\omega_{*i}}{\omega}\right)\tau\rho_i^2\nabla_\perp^2\phi \ , \qquad (1)$$

where ϕ and $A_{\parallel}$ are the perturbed electrostatic potential and the parallel vector potential, respectively, $k_{\parallel}$ is the parallel wave number, ω is the mode frequency, $\tau = T_e/T_i$, $\omega_* = (mcT/reB)(\partial \ \ell n \ N/\partial r)$, $\zeta_e = \omega/|k_{\parallel}|V_e$, $\rho_i^2 = T_i M_i (c/eB)^2$, m is the poloidal mode number, Z is the plasma dispersion function, and the subscripts refer to electrons and ions. The presence of alpha particles has a small effect on the neutrality condition but a large one on the current. To obtain a second relationship between ϕ and $A_\parallel$, we add together the parallel velocity moment of the gyroaveraged Vlasov equations for electrons, ions, and alpha particles. After some manipulation, with the help of the neutrality condition and Amperé's law, we obtain

$$\frac{1}{r^2}\left[\frac{\partial}{\partial r}\left(k_\parallel^2 r^3 \frac{\partial}{\partial r}\frac{A_\parallel}{rk_\parallel}\right) - (m^2 - 1)k_\parallel A_\parallel\right]$$

$$= \nabla_\perp\left\{\left[\frac{c}{V_A^2}(\omega - \omega_{*i}) - \frac{\beta_\alpha c\Gamma_{0\alpha}}{2\omega R^2} Z(\zeta_\alpha)\left(1 - \frac{\omega_{*\alpha}}{\omega}\right)\right]\nabla_\perp \phi\right\}$$

$$+ \frac{3}{4}\rho_i^2\nabla_\perp^2\left[\frac{c}{V_A^2}(\omega - \omega_{*i})\nabla_\perp^2\phi\right] , \qquad (2)$$

where $V_A^2 = B^2/4\pi N_i M_i$ is the Alfvén speed, $\zeta_\alpha = \omega/|k_\parallel|v_\alpha$, R is the major radius, and $\beta_\alpha = 8\pi N_\alpha T_\alpha/B^2$. In deriving Eq. (2), we have ignored the toroidal drifts for electrons and ions. The toroidal drift for the alpha particles leads to the term that is proportional to β_α on the right-hand side of Eq. (2). Details of the derivation are given in Appendix A. Equations (1) and (2) can be combined to obtain a single fourth-order eigenmode equation for cylindrical geometry:

$$\rho_i^2\left(\frac{1}{r^2}\frac{\partial}{\partial r} U_1 r^3 \frac{\partial}{\partial r}\frac{1}{r} - \frac{m^2 - 1}{r^2} U_1\right)\cdot\left(\frac{1}{r}\frac{\partial}{\partial r} r \frac{\partial}{\partial r} - \frac{m^2}{r^2}\right)\phi$$

$$+ \frac{1}{r^2}\frac{\partial}{\partial r} r^3 U_0 \frac{\partial}{\partial r}\frac{\phi}{r} - \frac{m^2 - 1}{r^2} U_0\phi = 0 , \qquad (3a)$$

where

$$U_0 = \frac{\omega^2}{V_A^2} - k_\parallel^2 - \beta_\alpha \left(1 - \frac{\omega_{*\alpha}}{\omega}\right) \frac{\zeta_\alpha Z(\zeta_\alpha)\Gamma_{0\alpha}}{2R^2} , \tag{3b}$$

and

$$U_1 = \frac{3\omega^2}{4V_A^2} + \frac{\tau k_\parallel^2}{1 + \zeta_e Z(\zeta_e)} . \tag{3c}$$

We note that Eq. (1) is equivalent to $\vec{E} + \vec{V} \times \vec{B} = 0$ if the finite Larmor radius term on the right-hand side is ignored, because $k_\parallel \phi - \omega A_\parallel /c$ is proportional to the parallel electric field. If this approximation is adopted, then Eq. (3) reduces to the second-order eigenmode equation derivable from magnetohydrodynamics. In Eq. (3), we have neglected ω_{*i} and ω_{*e} compared with ω, but $\omega_{*\alpha}$ is retained. Equation (3) is applicable to modes with poloidal mode number $m \geq 2$. (The $m = 1$ mode would require full toroidal geometry in the equilibrium.) The main difference between Eq. (3a) and the corresponding equation of Rosenbluth and Rutherford is in the finite Larmor radius terms. While Rosenbluth and Rutherford used a slab approximation for $\rho_i^2 \nabla_\perp^2$ terms, we keep their cylindrical form. This difference is important, as we shall see later, in that a quadratic form can be constructed from Eq. (3a) when β_α, $\zeta_e Z(\zeta_e) \to 0$, but not from the corresponding equation of Ref. 1.

When electron damping and alpha particle undamping are ignored, we can derive a quadratic form from Eqs. (1) and (2):

$$\omega^2\left[\int_0^a dr\,\frac{r^3}{V_A^2}\left|\frac{\partial}{\partial r}\frac{\phi}{r}\right|^2 + (m^2-1)\int_0^a dr\,\frac{|\phi|^2}{rV_A^2} - \frac{3}{4}\rho_i^2\int_0^a dr\,rV_A^{-2}\left|\left(\frac{1}{r}\frac{\partial}{\partial r}r\frac{\partial}{\partial r}-\frac{m^2}{r^2}\right)\phi\right|^2\right]$$

$$= \int_0^a dr\,k_\parallel^2 r^3\left|\frac{\partial}{\partial r}\frac{\phi}{r}\right|^2 + \int_0^a dr\,(m^2-1)k_\parallel^2\frac{|\phi|^2}{r}$$

$$+ \rho_s^2\int_0^a dr\,\frac{k_\parallel^2}{r^3}\left|\frac{\partial}{\partial r}r^3\frac{\partial}{\partial r}\frac{\phi}{r}\right|^2 + \rho_s^2\int_0^a dr\,k_\parallel^2\frac{|\phi|^2}{r^2}$$

$$+ 2\rho_s^2(m^2-1)\mathrm{Re}\left[\int_0^a dr\,k_\parallel^2 r^3\left(\frac{\partial}{\partial r}\frac{\phi^*}{r}\right)\left(\frac{\partial}{\partial r}\frac{\phi}{r^3}\right)\right], \quad (4)$$

where a is the minor plasma radius and ρ_s is the ion gyroradius with electron temperature. Derivation of Eq. (4) is given in Appendix B. For $m^2 > 1$, if $\rho_i/r \ll 1$, $\rho_i(\partial/\partial r) \ll 1$, and both sides of Eq. (4) are positive, ω^2 must be positive, and the system is neutrally stable. (The condition $k_r\rho_i \ll 1$ is necessary for the differential equation approach used here. The numerical solutions of Sec. III satisfy this condition well. Thus, the third term on the left-hand side of Eq. (4) is of $O(k_r^2\rho_i^2) \ll 1$ and cannot destabilize the kinetic Alfvén wave in the absence of fast particles.) However, if the finite Larmor radius terms in Eqs. (1) and (2) are approximated by their slab form, it is impossible to construct a quadratic form.

III. NUMERICAL SOLUTION

Equation (3) is solved numerically by a shooting code using a conducting wall boundary condition at r = a and $\tilde{E}_r = \tilde{B}_r = 0$ at r = 0, the magnetic axis. For tokamak geometry, $k_\parallel = (m - \ell q)/qR$, where ℓ is the toroidal mode number and q is the safety factor. We assume parabolic profiles for q and the density N,

$$q(r) = 1 + (q_a - 1)\left(\frac{r}{a}\right)^2$$

and

$$N = N_0\left[\rho_0 - \left(\frac{r}{a}\right)^2\right] \equiv N_0\rho \ .$$

In this section, we investigate the destabilization of the eigenmodes of the Alfvén wave ($\omega^2 = k_\parallel^2 V_A^2 \equiv \omega_A^2$) due to fast particles by choosing low mode numbers m,ℓ such that the first mode-rational surface $k_\parallel = 0$ lies radially outside of the Alfvén resonance $U_0 = 0$ [Eq. (3b)]. The term U_0 plays the role of a potential well for the radial eigenmodes. Figure 1 shows the normalized local shear Alfvén frequency, $k_\parallel/\rho^{1/2}$, for the modes shown in Figs. 2-4, where $k_\parallel = (m - \ell q)/q$. For the alpha particles, we assume

$$\beta_\alpha = \beta_{\alpha 0}\ \exp\left[-\left(\frac{r}{L_\alpha}\right)^2\right]$$

and

$$N_\alpha = N_{\alpha 0}\ \exp\left[-\left(\frac{r}{L_\alpha}\right)^2\right] .$$

When $\beta_{\alpha 0} = 0$ and electron Landau damping is turned off, for fixed ℓ and m such that $k_\parallel \neq 0$, we find radial eigenmodes with purely real ω. This confirms the conclusion from Eq. (4). The fundamental radial mode has both the smallest ω ($\omega/\omega_{A0} \sim 1$, where ω_{A0} is the Alfvén frequency at the center) and the Alfvén resonance surface closest to r = 0. As the radial mode number increases, ω increases and the Alfvén resonance surface moves outward. This outward movement of the Alfvén resonance surface is illustrated in Figs. 2-4, which show the fundamental, the second, and the sixth radial harmonics of the eigenmode for $\ell = 3$, $m = 2$, $a = 50$ cm, $\rho_0 = 1.1$, $q_a = 3$, and $\rho_i = 0.51$ cm. The normalized eigenfrequency $\Omega \equiv \omega R(4\pi N_0 M_i)^{1/2}/B_0$ increases as the radial mode number increases. Eigenmodes with frequencies exactly equal to the negative of those shown in Figs. 2-4 can be found. These modes correspond to the negative root of the local dispersion relation, $\omega = \pm k_{\|} V_A$. If the Rosenbluth and Rutherford version of Eq. (3a) is used, subject to the same boundary conditions and the same parameters as in Figs. 2-4, then unstable eigenmodes can be found numerically. An example of these unphysical radial eigenmodes is shown in Fig. 5.

When $\beta_{\alpha 0} \neq 0$ the neutrally stable eigenmodes of the exact equation are destabilized. The growth rate is largest for the fundamental mode and decreases with increasing radial mode number. The damping rate due to the electron resonance increases with increasing radial mode number. For appropriate values of $\beta_{\alpha 0}$, the combined effect of alpha particles and electron damping destabilizes these eigenmodes. Figure 6 shows the eigenfunctions of the unstable fundamental and second radial harmonics for the following parameters of an ignited tokamak: $\ell = -4$, $m = -3$, $q_a = 3$, $T_i = T_e = 10$ keV, $B = 45$ kG, $N_0 = 10^{14}/\text{cm}^3$, $\beta_i = \beta_e = 2\%$, $\beta_{\alpha 0} = 3\%$, $T_\alpha = 3.5$ MeV, $R = 4$ m, $a = 1$ m, $L_\alpha = 0.3$ m, and $\rho_0 = 1.1$. These parameters will now be varied.

Analyzing the local dispersion relation (discussed in Sec. IV), we see that this instability is driven by $\omega_{*\alpha}$. This is numerically confirmed in Fig. 7, where the growth rate Im Ω for the fundamental radial mode is plotted against L_α/a for T_α values of 3.5, 2.0, and 1 MeV. From Fig. 7, we conclude that (i) the growth rate is higher for larger T_α, (ii) it increases with decreasing L_α, and (iii) for fixed T_α, there exists a critical L_α below which the mode is unstable.

As mentioned, for each set of mode numbers there are two almost equal eigenfrequencies with opposite signs corresponding to the solutions $\omega = \pm k_\| V_A$ of the local dispersion relation. With $\beta_{\alpha 0} \neq 0$, one of the eigenmodes is destabilized. This branch is shown in Figs. 6 and 7. The other branch is damped by a nonzero $\beta_{\alpha 0}$, although it has almost the same eigenmode structure as the first branch. The difference in behavior of these two branches is illustrated by Table I, where the normalized eigenfrequencies Ω of these two branches are given for each set of ℓ, m, and n (radial mode number). To illustrate the stabilizing effect of the electron resonance, we list Ω for cases with and without electrons in separate columns. The parameters involved in Table I are the same as those for Fig. 6. We note also from Table I that there is a symmetry relation between the signs of ℓ, m, and Ω. This symmetry agrees with the prediction from the local dispersion to which we now turn in detail.

IV. LOCAL DISPERSION RELATION

In order to get a simple physical picture of the effects of alpha particles and electron resonance on the shear Alfvén eigenmodes, we derive the local dispersion relation from Eq. (3a) in the short radial wavelength limit ($\partial/\partial r = ik_r$, $k_r^2 >> m^2/r^2$, $k_\perp \cong k_r$):

$$\frac{\omega^2}{V_A^2}\left[1 - \frac{3}{4}(k_\perp \rho_i)^2\right] - \frac{\beta_a \Gamma_{0\alpha}}{2R^2}\left(1 - \frac{\omega_{*\alpha}}{\omega}\right)\zeta_{0\alpha} Z(\zeta)\alpha = k_\parallel^2\left[\frac{1 + \tau(k_\perp \rho_i)^2}{1 + \zeta_e Z(\zeta_e)}\right] . \tag{5}$$

Treating the β_α and the $\zeta_e Z(\zeta_e)$ terms as small, we can solve this dispersion relation to obtain

$$\omega = \omega_0 + \omega_\alpha + \omega_e , \tag{6a}$$

where

$$\omega_0 = \pm k_\parallel V_A \left[\frac{1 + \tau(k_\perp \rho_i)^2}{1 - 3/4(k_\perp \rho_i)^2}\right]^{1/2} ,$$

$$\omega_\alpha = \frac{\beta_\alpha \zeta_\alpha Z(\zeta_\alpha)(1 - \omega_{*\alpha}/\omega_0)V_A^2}{4R^2\omega_0[1 - 3(k_\perp \rho_i)^2/4]} \tag{6b}$$

$$\cong - \frac{\beta_\alpha \zeta_\alpha Z(\zeta_\alpha)\omega_{*\alpha} V_A^2 \Gamma_{0\alpha}}{4R^2\omega_0^2[1 - 3(k_\perp \rho_i)^2/4]} \tag{6c}$$

$$\omega_e = -(k_\parallel V_A)^2 \tau (k_\perp \rho_i)^2 \frac{\zeta_e Z(\zeta_e)}{2\omega_0} . \tag{6d}$$

Equation (6a) is the dispersion relation for the "kinetic" Alfvén wave of Hasegawa and Chen.[2] Obtaining the instability from the alpha contribution requires Im $\omega_\alpha > 0$. This is possible if $\overline{v}_\alpha > V_A$. Thus we expand $Z(\zeta_e)$ and $Z(\zeta_\alpha)$ in the small argument limit:

$$\omega_\alpha \cong - \frac{i\pi^{1/2}\beta_\alpha \Gamma_{0\alpha} V_A^2(\omega_{*\alpha}/\omega_0)}{4R^2|k_\parallel|v_\alpha[1 - 3(k_\perp \rho_i^2/4)]} , \tag{7a}$$

$$\omega_e \cong - \frac{i\pi^{1/2}(k_\parallel V_A)^2 \tau (k_\perp \rho_i)^2}{2|k_\parallel|V_e} . \tag{7b}$$

It follows from Eqs. (7a) and (7b) that the alpha particle contribution is destabilizing whenever ω_α^* and ω_0 have opposite signs. The electron resonance is always stabilizing. This conclusion agrees with results in Table I. Equations (6a), (7a), and (7b) explain our numerical results qualitatively, provided $k_\parallel$ is evaluated inside the region in which the eigenfunction decays exponentially. Thus, for eigenmodes with a low radial mode number, like those discussed in the preceding section, $k_\parallel$ is evaluated closer to the origin and is therefore smaller. Consequently the growth rate contributed by the alpha particles is larger and the electron damping is smaller. For higher radial mode numbers, the effective $k_\parallel$ is larger. Therefore, the growth rate contributed by the alpha particles is smaller and the electron resonance damping is larger, as observed in the preceding section.

V. ISLAND OVERLAPPING AND ANOMALOUS ALPHA DIFFUSION

As shown above, in a cylindrical tokamak with a sheared magnetic field, low mode number shear Alfvén waves can exist as a discrete set of radial eigenmodes $\phi_{\ell,m,n}$ with eigenfrequencies ω_n, with n = 0, 1, 2, . . ., where n counts the number of radial nodes between r = 0 and r = a. If energetic particles with average velocities greater than the Alfvén speed are introduced, eigenmodes $\phi_{\ell,m,n}$ with $0 \leq n \leq n_0$ are destabilized. Typically, n_0 is of the order of 10 for any one set of (ℓ,m). This is exemplified in Table II. Since $\omega_{n+1} - \omega_n << \omega_n$, the radial spacing for adjacent Alfvén resonances,

$$\omega_n = k_\parallel(r_n)V_A(r_n) \; ,$$

with n = 0, 1, 2 . . ., can be very small. This suggests the possibility of island overlapping and stochastic diffusion of the destabilizing alpha particles, and thus of flattening the rather peaked alpha particle density profile at birth. In this section, we estimate the minimum fluctuation level that causes island overlap and the corresponding stochastic alpha particle diffusion coefficient at this fluctuation level, which turns out to be quite low ($e_i\phi/T_i \gtrsim 0.05$). At threshold, we find a radial diffusion coefficient of $D_r^\alpha \gtrsim 4.4 \times 10^3$ cm/s, indicating a short alpha ($\bar{v}_\alpha > V_A$) confinement time of the background plasma; this is, however, sufficiently long to permit slowing down of the scattered alpha particles in the outer region of the background plasma.

Following standard procedure,[4,5] the perturbed orbit equations for the alpha particles are

$$\frac{d}{dt}\,\delta r = -\frac{c}{B}\frac{J_0}{r}\frac{\partial}{\partial\theta}\left(\phi - \frac{v_\parallel}{c}A_\parallel\right) \tag{8a}$$

and

$$\frac{d}{dt}\,\delta\theta = -\frac{v_\parallel}{Rq}\frac{\partial\ \ell n\ q}{\partial r}\,\delta r + \frac{c}{B}\frac{J_0}{r}\frac{\partial}{\partial r}\left(\phi - \frac{v_\parallel}{c}A_\parallel\right)\ , \tag{8b}$$

where J_0 is the Bessel function and one can drop the piece $v_\parallel A_\parallel/c$ for alpha particles ($V_\parallel/c << 1$). A Hamiltonian can be found,

$$H = -\frac{(\delta r)^2}{2}\frac{v_\parallel}{Rq}\frac{\partial\ \ell n\ q}{\partial r} + \frac{c}{B}\frac{J_0}{r}\left(\phi - \frac{v_\parallel}{c}A_\parallel\right)\ , \tag{9a}$$

so that the perturbed orbit equations can be written as

$$\frac{d}{dt}\,\delta r = -\frac{\partial H}{\partial\delta\theta}$$

and

$$\frac{d}{dt}\,\delta\theta = \frac{\partial H}{\partial\delta r}\ . \tag{9b}$$

The dependence of H on $\delta\theta$ occurs through the fluctuating fields. From Eq. (9a) the island width is approximately

$$\Delta_I^2 \sim 2cJ_0|\phi|Rq\left(v_\alpha Br\,\frac{\partial\ \ell n\ q}{\partial r}\right)^{-1}\ , \tag{10}$$

with all quantities evaluated at $r = r_n$.

The radial spacing for the closely adjacent Alfvén resonances is given by $\Delta n \equiv r_{n+1} - r_n$,

$$\Delta_n = 2\delta\omega_n \cdot \omega_n \Big/ \frac{\partial}{\partial r_n} [k_\parallel^2(r_n) V_A^2(r_n)] \ . \tag{11}$$

Island overlap occurs when $\Delta_I > \Delta_n$, which is equivalent to

$$\frac{e_i\phi}{T_i} \geqslant \frac{0.5v_\alpha}{J_0 Rq}\left(\frac{cT_i}{e_i B}\,\frac{1}{a^2}\right)^{-1} \frac{\partial \ \ell n \ q}{\partial \ \ell n \ r}\left(\frac{\Delta_n}{a}\right)^2 , \tag{12}$$

where the logarithmic derivative is evaluated at the n = 0 Alfvén resonance, which is typically at r_0 = 10 cm.

In Table II, we show two sets of unstable modes with the radial location of their Alfvén resonances. The first set consists of modes with $\ell = -3$, $m = -2$, the second with $\ell = -4$, $m = -3$. The parameters used are those of Fig. 6, except L_α = 0.4 m. From the eigenfrequencies of these modes, the location of their Alfvén resonances is found numerically, and so is the spacing between adjacent resonance surfaces. The largest spacing, which in this case is 2.4 cm, occurs when the radial mode number n is low. Using these parameters, we obtain for the minimum fluctuation level at the threshold of island overlap a value of $e_i\phi/T_i \gtrsim 0.05$, which is not unreasonable even for the present drift-Alfvén-type tokamak turbulence.[6]

An estimate for the radial diffusion coefficient at threshold for the alpha particles can be obtained by using[7]

$$D_r = \int_{-\infty}^{t} dt' \langle \delta\dot{r}(t')\delta\dot{r}(t)\rangle \ .$$

With $\delta\dot{r} = -(cJ_0/rB)\partial\phi/\partial\theta$, one obtains

$$D_r \sim \tau_c \left(\frac{c}{B}\right)^2 (J_0 k_\theta |\phi|)^2 \gtrsim \tau_c \left(\frac{v_\alpha \Delta_n}{2Rq}\right)^2 \left(k_\theta \Delta_n \frac{\partial \ \ln q}{\partial \ \ln r}\right)^2 ,$$

where τ_c is the correlation of time for the fluctuations.

Using $\tau_c \gtrsim 1/\omega$, we estimate the diffusion coefficient for the above example to be $D_r \gtrsim 4.4 \times 10^3$ cm^2/s, which corresponds to an alpha confinement time of $\tau_\alpha \sim a^2/4D_r \lesssim 1.1$ s.

Appendix A

For simplicity, the tokamak geometry is modeled by a cylinder for the electron and ion species. Within this context, toroidal magnetic gradient and curvature drifts for the electrons and ions, as well as the poloidal mode coupling, are ignored. For alpha particles, the toroidal magnetic gradient and curvature drifts must be retained because of their high energy. However, the poloidal mode coupling induced by these drifts is still neglected. A more complete treatment retaining the full features of toroidal geometry is beyond the scope of the present study. The perturbed ion distribution function f_i is related to the perturbed scalar potential ϕ and the parallel component of vector potential A through the linearized Vlasov equation, which (after it is averaged over the gyrophase angle ϕ) can be written as

$$(\omega - k_\parallel v_\parallel)g_i = \frac{e}{T_i}(\omega - \omega_{*i})F_i J_0\left(\phi - \frac{v_\parallel}{c} A_\parallel\right) , \qquad (A.1)$$

where $f_i = -(e\phi/T_i)F_i + \exp(iL)g_i$, $L = (k_\perp v_\perp/\Omega_i)\cos\phi$, $\vec{k}_\perp = -i\vec{\nabla}_\perp$, and all perturbed quantities have assumed the form $\exp(-i\omega t + im\theta - i\ell\zeta)$.

In Eq. (A.1), $F_i = N(M_i/2\pi T_i)^{3/2}\exp(-M_i v^2/2T_i)$ is the equilibrium ion distribution function, $\omega_{*i} = (m/r)(cT_i/eB)(\partial \ln N_i/\partial r)$, $V_\parallel$ is the parallel velocity, $J_0 = J_0(v_\perp k_\perp/\Omega_i)$ is the zeroth-order Bessel function, Ω_i is the ion gyrofrequency, $k_\parallel = (m - \ell q)/Rq$, R is the major radius, and q is the safety factor. We have also ignored $|\vec{\nabla}_\perp N|$ compared with $|\vec{\nabla}_\perp \phi|$. The perturbed ion density N_i is, therefore, assuming $\omega >> k_\parallel v_i$,

$$\frac{\tilde{N}_i}{N_i} = \frac{e}{T_i}\left[-1 + \left(1 - \frac{\omega_{*i}}{\omega}\right)\Gamma_0\right]\phi \ , \tag{A.2}$$

where $\Gamma_0 = I_0(b)\exp(-b)$, $b = 1/2(v_i k_\perp/\Omega_i)^2$, and $v_i^2 = 2T_i/M_i$.

For electrons, we need to take into account the equilibrium current u. The nonadiabatic electron response $g_e = f_e - (e\phi/T_e)F_e$ satisfies

$$(\omega - k_\parallel v_\parallel)g_e = -\frac{e}{T_e} F_e(\omega - \omega_{*e}^u)\left(\phi - \frac{v_\parallel}{c} A_\parallel\right) \ , \tag{A.3}$$

where

$$\omega_{*e}^u = -\frac{m}{r}\frac{cT_e}{eB}\left[\frac{N_e'}{N_e} + \frac{M(v_\parallel - u)}{T_e} u'\right] \ ,$$

$N' = \partial N/\partial r$, and $u' = \partial u/\partial r$.

The perturbed electron density can be readily calculated:

$$\frac{\tilde{N}_e}{N_e} = \frac{e\phi}{T_e} - \frac{e}{T_e}\frac{\omega - \omega_{*e}}{k_\parallel c} A_\parallel + \frac{e}{T_e}\left(1 - \frac{\omega_{*e}}{\omega}\right)\zeta_e Z(\zeta_e)\left(\phi - \frac{\omega A_\parallel}{k_\parallel c}\right) , \tag{A.4}$$

where

$$Z(\zeta) = \pi^{-1/2}\int_{-\infty}^{+\infty} \frac{e^{-t^2}\,dt}{t - \zeta}$$

is the plasma dispersion function and $\zeta_e = \omega_e/|k_\parallel|v_e$. If we assume that the equilibrium distribution of the alpha particles is a Maxwellian with temperature T_α, then the perturbed alpha density can be obtained in a manner similar to that used for the ions. However, we now have $\omega \sim k_\parallel V_A$. The perturbed alpha density can be written as

$$\frac{\tilde{N}_\alpha}{N_\alpha} = \frac{Z_\alpha e}{T_\alpha}\left[-\phi + \frac{\omega - \omega_{*\alpha}}{k_\parallel c} A_\parallel \Gamma_{0\alpha} - \Gamma_{0\alpha}\frac{\omega - \omega_{*\alpha}}{\omega - \omega_{d\alpha}}\left(\phi - \frac{\omega - \omega_{d\alpha}}{k_\parallel c} A_\parallel\right)\zeta_\alpha Z(\zeta_\alpha)\right] , \tag{A.5}$$

where $\omega_{*\alpha} = mcT_\alpha N_\alpha'/rZ_\alpha eBN_\alpha$, $\zeta_\alpha = (\omega - \omega_{d\alpha})/|k_\parallel|v_\alpha$, $\omega_{d\alpha} = \vec{V}_{d\alpha} \cdot \vec{\nabla}$, $\vec{V}_{d\alpha} \cong c\varepsilon_\alpha(Z_\alpha eBR)^{-1}(\cos\theta\hat{\theta} + \sin\theta\hat{r})$, $\Gamma_{0\alpha} = I_0(b_\alpha)\exp(-b_\alpha)$, $b_\alpha = 1/2(v_\alpha k_\perp/\Omega_\alpha)^2$, $\Omega_\alpha = Z_\alpha eB/M_\alpha c$, and Z_α is the atomic number for the alphas.

From Eqs. (A.2), (A.4), and (A.5), we obtain the first relationship between ϕ and $A_\parallel$ using the neutrality condition. Expanding Γ_0 for ions in the small argument limit, we have

$$\left(1 - \frac{\omega_{*e}}{\omega}\right)\left(\phi - \frac{\omega A_\parallel}{k_\parallel c}\right)[1 + \zeta_e Z(\zeta_e)] = \frac{N_i T_e}{N_e T_i}\left(1 - \frac{\omega_{*i}}{\omega}\right)\rho_i^2\nabla_\perp^2\phi$$

$$- \frac{N_\alpha Z_\alpha^2}{N_e}\frac{T_e}{T_\alpha}\left(1 - \frac{\omega_{*\alpha}}{\omega}\right)\left\{\phi\left[1 + \frac{\omega}{\omega - \omega_{d\alpha}}\Gamma_{0\alpha}\zeta_\alpha Z(\zeta_\alpha)\right] - \frac{\omega A_\parallel}{k_\parallel c}\Gamma_{0\alpha}[1 + \zeta_\alpha Z(\zeta_\alpha)]\right\} . \tag{A.6}$$

Since $N_\alpha << N_e$ and $T_e << T$, we can approximate Eq. (A.6) by

$$\left(1 - \frac{\omega_{*e}}{\omega}\right)\left(\phi - \frac{\omega A_\parallel}{k_\parallel c}\right)[1 + \zeta_e Z(\zeta_e)] \cong \left(1 - \frac{\omega_{*i}}{\omega}\right)\tau\rho_i^2\nabla_\perp^2\phi . \tag{A.7}$$

Thus the presence of alpha particles has little effect on the neutrality condition. To obtain the second relationship between ϕ and $A_\parallel$, we take the moments of Eqs. (A.1) and (A.3) and the corresponding moment for alpha particles:

$$\int d\vec{V}(\omega - k_\parallel v_\parallel)\exp(iL)g_i = \frac{e}{T_i}(\omega - \omega_{*i})N_i\Gamma_0\phi \ , \tag{A.8a}$$

$$\int d\vec{V}(\omega - k_\parallel v_\parallel)g_e = \frac{-e}{T_e}\phi N_e(\omega - \omega_{*e}) + \frac{eA_\parallel}{cT_e}N_e u\omega + \frac{mA_\parallel(N_e u)'}{rB} \ , \tag{A.8b}$$

$$\int d\vec{V}(\omega - k_\parallel v_\parallel - \vec{V}_{d\alpha}\cdot\vec{\nabla})\exp(iL_\alpha)g_\alpha = \frac{Z_\alpha eN_\alpha}{T_\alpha}(\omega - \omega_{*\alpha})\Gamma_{0\alpha}\phi \ . \tag{A.8c}$$

With the help of the exact neutrality condition,

$$\frac{-e\phi N_i}{T_i} + \int g_i\exp(iL)d\vec{V} - \frac{Z_\alpha^2 e\phi N_\alpha}{T_\alpha} + Z_\alpha\int g_\alpha\exp(iL_\alpha)d\vec{V} = \frac{e\phi N_e}{T_e} + \int g_e d\vec{v} \ ,$$

we can combine the variations in Eq. (A.8) to get

$$k_\parallel\left(\tilde{j}_\parallel + \frac{e^2\phi N_e u}{T_e}\right) - \frac{e^2A_\parallel N_e u\omega}{cT_e} + \frac{mA_\parallel J_\parallel'}{rB} = e^2\phi\left[\frac{N_i}{T_i}(\omega - \omega_{*i})(1 - \Gamma_0)\right.$$

$$\left. + \frac{Z_\alpha^2 N_\alpha}{T_\alpha}(\omega - \omega_{*\alpha})(1 - \Gamma_{0\alpha})\right] - Z_\alpha e\int\exp(iL_\alpha)\vec{V}_{d\alpha}\cdot\vec{\nabla}g_\alpha d\vec{V} \ , \tag{A.9}$$

where

$$\tilde{j}_\parallel = e\int v_\parallel[\exp(iL)g_i + \exp(iL_\alpha)g_\alpha - g_e]d\vec{V} - \frac{e^2\phi N_e u}{T_e}$$

and $J_\parallel = -eN_e u$ is the equilibrium parallel current. Using Ampere's law and the large aspect ratio expansion, we can show

$$k_{\parallel}\tilde{j}_{\parallel} + \frac{mA_{\parallel}J_{\parallel}'}{rB} = -\frac{c}{4\pi r^2}\left[\frac{\partial}{\partial r}\left(k_{\parallel}^2 r^3 \frac{\partial}{\partial r}\frac{A_{\parallel}}{rk_{\parallel}}\right) - (m^2 - 1)k_{\parallel}A_{\parallel}\right] .$$

Therefore, Eq. (A.10) becomes

$$\frac{1}{r^2}\left[\frac{\partial}{\partial r}\left(k_{\parallel}^2 r^3 \frac{\partial}{\partial r}\frac{A_{\parallel}}{rk_{\parallel}}\right) - (m^2 - 1)k_{\parallel}A_{\parallel}\right] - \frac{4\pi e^2 N_e}{cT_e} uk_{\parallel}\left(\phi - \frac{\omega A_{\parallel}}{k_{\parallel}c}\right)$$

$$= -\frac{4\pi e^2\phi}{c}\left[\frac{N_i}{T_i}(\omega - \omega_{*i})(1 - \Gamma_0) + \frac{Z_{\alpha}^2 N_{\alpha}}{T_{\alpha}}(\omega - \omega_{*\alpha})(1 - \Gamma_{0\alpha})\right]$$

$$+ \frac{4\pi Z_{\alpha}e}{c}\int \exp(iL_{\alpha})\vec{V}_{d\alpha} \cdot \vec{\nabla} g_{\alpha} d\vec{V} . \quad \text{(A.10)}$$

Since $N_i/T_i >> N_{\alpha}/T_{\alpha}$, we can ignore the $\omega - \omega_{*\alpha}$ term in the square bracket on the right-hand side of the equation. Thus the largest term due to alpha particles is the $\vec{V}_{d\alpha} \cdot \vec{\nabla} g_{\alpha}$ term,

$$I \equiv \int \exp(iL_{\alpha})\vec{V}_{d\alpha} \cdot \vec{\nabla} g_{\alpha} d\vec{v} = \int \exp(iL_{\alpha})\vec{V}_{d\alpha}$$

$$\cdot \vec{\nabla} \frac{\omega - \omega_{*\alpha}}{\omega - k_{\parallel}v_{\parallel} - \omega_{d\alpha}} F_{\alpha}J_{0\alpha}\left(\phi - \frac{v_{\parallel}}{c}A_{\parallel}\right)\frac{Z_{\alpha}e}{T_{\alpha}} .$$

Expanding in $\omega_{d\alpha}$,[9] we can perform the integral to obtain

$$I = -\frac{Z_{\alpha}e}{T_{\alpha}}\frac{N_{\alpha}}{\omega}\Gamma_{0\alpha}\vec{V}_{d\alpha} \cdot \vec{\nabla}\left(1 - \frac{\omega_{*\alpha}}{\omega}\right)\vec{V}_{d\alpha} \cdot \vec{\nabla}\left\{Z\zeta_{0\alpha}^2[1 + \zeta_{0\alpha}Z(\zeta_{0\alpha})]\right.$$

$$\left.\cdot\left(\phi - \frac{\omega A_{\parallel}}{k_{\parallel}c}\right) + \zeta_{0\alpha}Z(\zeta_{0\alpha})\frac{\omega A_{\parallel}}{k_{\parallel}c}\right\} \cong -\frac{Z_{\alpha}e}{T_{\alpha}}\frac{N_{\alpha}}{\omega}\Gamma_{0\alpha}V_{d\alpha}^2\nabla_{\perp}^2\phi\zeta_{0\alpha}Z(\zeta_{0\alpha})\left(1 - \frac{\omega_{*\alpha}}{\omega}\right) ,$$

where $\zeta_{0\alpha} = \omega/|k_{\parallel}|v_{\alpha}$ and $V_{d\alpha} = cT_{\alpha}(Z_{\alpha}eBR)^{-1}$.

In evaluating the integral I, we have ignored all terms that lead to coupling of different m modes and used the approximated relationship $\phi \cong \omega A_\parallel / k_\parallel c$ from the neutrality condition because the difference is of order $(k_\perp \rho_i)^2$. Equation (A.10) can therefore be written as

$$\frac{1}{r^2}\left[\frac{\partial}{\partial r}\left(k_\parallel^2 r^3 \frac{\partial}{\partial r}\frac{A_\parallel}{r k_\parallel}\right) - (m^2 - 1)k_\parallel A_\parallel\right] = \nabla_\perp\left\{\left[\frac{c}{V_A^2}(\omega - \omega_{*i}) - \frac{B_\alpha \Gamma_{0\alpha} c}{Z\omega R^2}\zeta_{0\alpha} Z(\zeta_{0\alpha})\right.\right.$$

$$\left.\left.\cdot\left(1 - \frac{\omega_{*\alpha}}{\omega}\right)\right]\nabla_\perp \phi\right\} + \frac{3}{4}\rho_i^2 \nabla_\perp^2 \left[\frac{c}{V_A^2}(\omega - \omega_{*i})\nabla_\perp^2 \phi\right], \qquad \text{(A.11)}$$

where $V_A^2 = B^2/(4\pi N_i M_i)$ is the Alfvén speed and $\beta_\alpha = 8\pi N_\alpha T_\alpha / B^2$.

In deriving Eq. (A.11), we have expanded Γ_0 in small b limit and ignored the current-driven term because u/c is very small. If the ρ_i^2 and β_α terms in Eqs. (A.8b) and (A.11) are ignored, we get

$$\frac{1}{r^2}\frac{\partial}{\partial r} r^3 \left[\frac{\omega(\omega - \omega_{*i})}{V_A^2} - k_\parallel^2\right]\frac{\partial}{\partial r}\frac{\phi}{r} - \frac{m^2 - 1}{r^2}\left[\frac{\omega(\omega - \omega_{*i})}{V_A^2} - k_\parallel^2\right]\phi = 0 \ , \qquad \text{(A.12)}$$

which is the ideal MHD equation describing the shear Alfvén wave in cylindrical geometry, including the effect of ω_{*i}. However, without sharp equilibrium gradients, an eigenmode equation of this type admits only the continuous spectrum.[8] For the shear Alfvén wave, $\omega \sim k_\parallel V_A >> \omega_{*i}$, we can ignore ω_{*i} compared with ω.

The resulting eigenmode equations are:

$$[1 + \zeta_e Z(\zeta_e)]\left(\phi - \frac{\omega A_\parallel}{k_\parallel c}\right) = \tau \rho_i^2 \nabla_\perp^2 \phi \qquad \text{(A.13a)}$$

and

$$\frac{1}{r^2}\left[\frac{\partial}{\partial r}\left(k_\parallel^2 r^3 \frac{\partial}{\partial r}\frac{A_\parallel}{rk_\parallel}\right) - (m^2 - 1)k_\parallel A_\parallel\right] = \frac{1}{r^2}\frac{\partial}{\partial r}\left(r^3 U \frac{\partial}{\partial r}\frac{\phi}{r}\right)$$

$$- \frac{m^2 - 1}{r^2} U\phi + \frac{3}{4}\rho_i^2 \nabla_\perp^2 \frac{c\omega}{V_A^2} \nabla_\perp^2 \phi \ , \quad \text{(A.13b)}$$

where

$$\nabla_\perp^2 = \frac{1}{r}\frac{\partial}{\partial r} r \frac{\partial}{\partial r} - \frac{m^2}{r^2}$$

and

$$U = \frac{c\omega}{V_A^2} - \frac{\beta_\alpha \Gamma_{0\alpha} c}{2\omega R^2} \zeta_{0\alpha} Z(\zeta_{0\alpha})\left(1 - \frac{\omega_{*\alpha}}{\omega}\right).$$

Equations (A.13a) and (A.13b) can be written as a single fourth-order equation, namely, Eq. (3a) in the main text.

Appendix B

We introduce $\psi = \omega A_{\parallel}/k_{\parallel} c$ and rewrite Eqs. (A.13a) and (A.13b) as

$$\phi - \psi = \rho_s^2 \left(\frac{1}{r}\frac{\partial}{\partial r} r \frac{\partial}{\partial r} - \frac{m^2}{r^2}\right)\phi \tag{B.1a}$$

and

$$\frac{1}{r^2}\left[\frac{\partial}{\partial r} k_{\parallel}^2 r^3 \frac{\partial}{\partial r}\frac{\psi}{r} - (m^2 - 1)k_{\parallel}^2\psi\right] = \frac{1}{r^2}\frac{\partial}{\partial r} r^3 \frac{\omega^2}{V_A^2}\frac{\partial}{\partial r}\frac{\phi}{r} - \frac{m^2 - 1}{r^2}\frac{\omega^2}{V_A^2}\phi$$

$$+ \frac{3}{4}\rho_i^2\left(\frac{1}{r}\frac{\partial}{\partial r} r \frac{\partial}{\partial r} - \frac{m^2}{r^2}\right)\frac{\omega^2}{V_A^2}\left(\frac{1}{r}\frac{\partial}{\partial r} r \frac{\partial}{\partial r} - \frac{m^2}{r^2}\right)\phi \ , \tag{B.1b}$$

where the limit $\beta_\alpha \to 0$ and $\zeta_e z(\zeta_e) \to 0$ has been taken.

If we multiply Eq. (B.1b) by $r\phi^*$ and integrate over r from 0 to a (where ϕ^* is the complex conjugate of ϕ), we get

$$\int_0^a dr\ k_{\parallel}^2 r^3 \left(\frac{\partial}{\partial r}\frac{\phi^*}{r}\right)\left(\frac{\partial}{\partial r}\frac{\psi}{r}\right) + (m^2 - 1)\int_0^a dr\ k_{\parallel}^2 \frac{\phi^*\psi}{r}$$

$$= \int_0^a dr\ r^3 \frac{\omega^2}{V_A^2}\left|\frac{\partial}{\partial r}\frac{\phi}{r}\right|^2 + (m^2 - 1)\int_0^a dr\ \frac{\omega^2}{V_A^2}\frac{|\phi|^2}{r}$$

$$- \frac{3}{4}\rho_i^2 \int_0^a dr\ \frac{\omega^2 r}{V_A^2}\left|\left(\frac{1}{r}\frac{\partial}{\partial r} r \frac{\partial}{\partial r} - \frac{m^2}{r^2}\right)\phi\right|^2 \ , \tag{B.2}$$

after integrating by parts and using the boundary conditions to get rid of the boundary terms. If all finite Larmor radius terms are ignored, we easily get

$$\omega^2 \left[\int_0^a \frac{r^3}{V_A^2} \left| \frac{\partial}{\partial r} \frac{\phi}{r} \right|^2 + (m^2 - 1) \int_0^a dr \frac{|\phi|^2}{rV_A^2} \right]$$

$$= \int_0^a dr\, k_\parallel^2 r^3 \left| \frac{\partial}{\partial r} \frac{\phi}{r} \right|^2 + (m^2 - 1) \int_0^a dr\, k_\parallel^2 \frac{|\phi|^2}{r} . \quad \text{(B.3)}$$

This corresponds to the quadratic form obtained from the second-order equation, which implies that ω^2 of the second-order equation is always real and positive if those integrals in Eq. (B.3) exist.

When the finite Larmor radius terms are retained, the difficulty is to show that the left-hand side of Eq. (B.2) is still real and positive. Using Eq. (B.1a), we have

$$\int_0^a dr\, k_\parallel^2 r^3 \left(\frac{\partial}{\partial r} \frac{\phi^*}{r}\right)\left(\frac{\partial}{\partial r} \frac{\psi}{r}\right) = \int_0^a dr\, k_\parallel^2 r^3 \left| \frac{\partial}{\partial r} \frac{\phi}{r} \right|^2 + \rho_s^2 \int dr\, k_\parallel^2 r^3 \left(\frac{\partial}{\partial r} \frac{\phi^*}{r}\right)$$

$$\cdot \frac{\partial}{\partial r}\left(\frac{m^2 - 1}{r^3} \phi\right) + \rho_s^2 \int_0^a dr \frac{k_\parallel^2}{r^3} \left| \frac{\partial}{\partial r} r^3 \frac{\partial}{\partial r} \frac{\phi^*}{r} \right|^2$$

and

$$\int_0^a dr\, k_\parallel^2 \frac{\phi^*\psi}{r} = \int_0^a dr\, k_\parallel^2 \frac{|\phi|^2}{r} + \rho_s^2 (m^2 - 1) \int_0^a dr \frac{k_\parallel^2}{r^2} |\phi|^2$$

$$+ \rho_s^2 \int_0^a dr\, k_\parallel^2 \left(\frac{\partial}{\partial r} \frac{\phi^*}{r^3}\right) r^3 \left(\frac{\partial}{\partial r} \frac{\phi}{r}\right) ,$$

where terms with $\partial k_\parallel^2/\partial r$ have been dropped because $\partial k_\parallel/\partial r \ll \partial\phi/\partial r$, as is borne out by our nummerical results. Therefore, Eq. (B.2) can be written as

$$\omega^2\left[\int_0^a dr\,\frac{r^3}{V_A^2}\left|\frac{\partial}{\partial r}\frac{\phi}{r}\right|^2 + (m^2-1)\int_0^a dr\,\frac{|\phi|^2}{rV_A^2} - \frac{3}{4}\rho_i^2\int_0^a dr\,rV_A^{-2}\right.$$

$$\left.\cdot\left|\left(\frac{1}{r}\frac{\partial}{\partial r}r\frac{\partial}{\partial r} - \frac{m^2}{r^2}\right)\phi\right|^2\right] = \int_0^a dr\,k_\parallel^2 r^3\left|\frac{\partial}{\partial r}\frac{\phi}{r}\right|^2 + \int_0^a dr(m^2-1)k_\parallel^2\,\frac{|\phi|^2}{r}$$

$$+\,\rho_s^2\int_0^a dr\,\frac{k_\parallel^2}{r^3}\left|\frac{\partial}{\partial r}r^3\frac{\partial}{\partial r}\frac{\phi}{r}\right|^2 + \rho_s^2(m^2-1)^2\int_0^a dr\,k_\parallel^2\,\frac{|\phi|^2}{r^2}$$

$$+\,2\rho_s^2(m^2-1)\,\mathrm{Re}\left[\int_0^a dr\,k_\parallel^2 r^3\left(\frac{\partial}{\partial r}\frac{\phi^*}{r}\right)\left(\frac{\partial}{\partial r}\frac{\phi}{r^3}\right)\right] \quad . \qquad (B.4)$$

Both the right-hand side of Eq. (B.4) and the square bracket multiplied by ω^2 are real. Therefore, ω^2 must be real. Furthermore, under normal conditions $\{\rho_i^2/r^2$ or $[\rho_i(\partial/\partial r)]^2 \ll 1\}$ necessary to justify the differential equation approach used in this paper and also borne out by our numerical results, the positive definite terms on both sides of Eq. (B.4) do not change signs because of the presence of the other terms. Hence, ω^2 must be positive.

ACKNOWLEDGMENTS

D. J. Sigmar would like to thank A. Mikhailovski and T. Kaladze for discussions of this problem and for directing his interest to the question of Alfvén waves as radial eigenmodes in sheared geometry. The authors would also like to thank S. P. Hirshman, who provided many stimulating suggestions throughout the course of this work, and R. J. Hastie, J. Freidberg, and G. Vahala for their fruitful comments on the ideal Alfvén wave spectrum.

REFERENCES

[1]M. N. Rosenbluth and P. H. Rutherford, Phys. Rev. Lett. 34, 1428 (1975).

[2]A. Hasegawa and L. Chen, Phys. Rev. Lett. 35, 370 (1975).

[3]A. B. Mikhailovskii, Zh. Eksp. Teor. Fiz. 68, 1772 (1975).

[4]G. R. Smith and A. Kaufman, Phys. Fluids 21, 2230 (1978).

[5]K. Molvig, private communication. We gratefully acknowledge his outline of the derivation leading to Eq. (12).

[6]This low value for the onset of alpha particle stochasticity suggests that the calculation of the self-consistent fluctuation level, which will be the subject of a subsequent paper, is worthwhile.

[7]P. E. Hall and P. A. Sturrock, Phys. Fluids 10, 2620 (1967).

[8]L. D. Pearlstein and J. P. Freidberg, Phys. Fluids 21, 1218 (1978).

[9]We have tacitly performed here a transit average that in this case is the same as as average in ϕ because the alpha particle velocity is much higher than the Alfvén speed. Coupling to sidebands is thus eliminated. In contrast, Ref. 1 has to rely on sideband coupling to excite instability.

TABLE I. Real and imaginary parts of the normalized eigenfrequency with and without the electron resonance.

			With α and electron resonance		With α resonance only	
ℓ	m	n	Re Ω	Im Ω	Re Ω	Im Ω
-3	-2	1	0.9956	0.0008	0.9910	0.0110
			-1.0067	-0.0157	-1.0068	-0.0132
		2	1.0156	0.0006	1.0159	0.0103
			-1.0309	-0.0164	-1.0310	-0.0124
		3	1.0162	0.0138	1.0165	0.0175
			-1.0330	-0.0151	-1.0331	-0.0114
		14	1.2359	-0.0025	1.2370	0.0132
			-1.2503	-0.0233	-1.2509	-0.0078
3	2	1	1.0067	-0.0157	1.0068	-0.0132
			-0.9956	0.0008	-0.9910	0.0110
		2	1.0309	-0.0164	1.0310	-0.0124
			-1.0156	0.0006	-1.0159	0.0103

TABLE II. Normalized locations r_n/a and spacings Δ_n/a for the Alfvén resonance surfaces of various unstable radial eigenmodes for $\ell = -3$, $m = -2$, and $\ell = -4$, $m = -3$.[a]

$-\ell$	$-m$	Re Ω	Im Ω	r_n/a	Δ_n/a
3	2	0.9908	0.0084	0.0943	0.0009
4	3	1.0090	0.01275	0.0952	0.0237
4	3	1.0390	0.0099	0.1189	0.0032
3	2	1.0160	0.0063	0.1221	0.0169
4	3	1.0690	0.0071	0.1390	0.0061
3	2	1.0410	0.0042	0.1451	0.0119
4	3	1.1000	0.0044	0.1570	0.0083
3	2	1.0660	0.0021	0.1653	0.0082
4	3	1.1310	0.0016	0.1735	0.0102
3	2	1.0910	0.0000	0.1837	0.0052
4	3	1.1630	0.0011	0.1889	

[a]The parameters used are those of Fig. 6.

FIGURE CAPTIONS

FIG. 1. The normalized local shear Alfvén frequency $k_{\parallel}/\rho^{1/2}$ as a function of the minor radius r for $\ell = 3$, $m = 2$, $q(a) = 3$, $a = 50$ cm, and $\rho_o = 1.1$.

FIG. 2. The fundamental radial eigenmode ($n = 1$) for $\ell = 3$, $m = 2$, $q(a) = 3$, $a = 50$ cm, $\rho_o = 1.1$, and $\rho_i = 0.51$ cm. The normalized eigenfrequency is $\omega/\omega_{A0} \equiv \Omega = \pm 1.0976$.

FIG. 3. The second radial harmonic eigenmode ($n = 2$) for the same parameters as in Fig. 2, $\Omega = \pm 1.1789$.

FIG. 4. Sixth radial harmonic eigenmode ($n = 6$) for the same parameters as in Fig. 2, $\Omega = \pm 1.5269$.

FIG. 5. An example of an unstable eigenmode of the Rosenbluth-Rutherford slab geometry equation subjected to the same boundary conditions and the same limit, and with the same parameters as in Figs. 2-4, $\Omega = 1.7149 + 0.0359i$.

FIG. 6. The eigenfunctions (Re ϕ/r) of the unstable fundamental (Fig. 1a) and first radial (Fig. 1b) harmonic for $\ell = -4$, $m = -3$ for the parameters of an ignited tokamak, as given in the text. The eigenfrequencies are $\Omega = 1.009 + i0.013$ and $1.039 + i0.010$, respectively.

FIG. 7. The normalized growth rate Im Ω for the fundamental radial mode vs normalized proportional particle density scale length L_α/a for $T_\alpha = 3.5$, 2, and 1 MeV. Same parameters as Fig. 6.

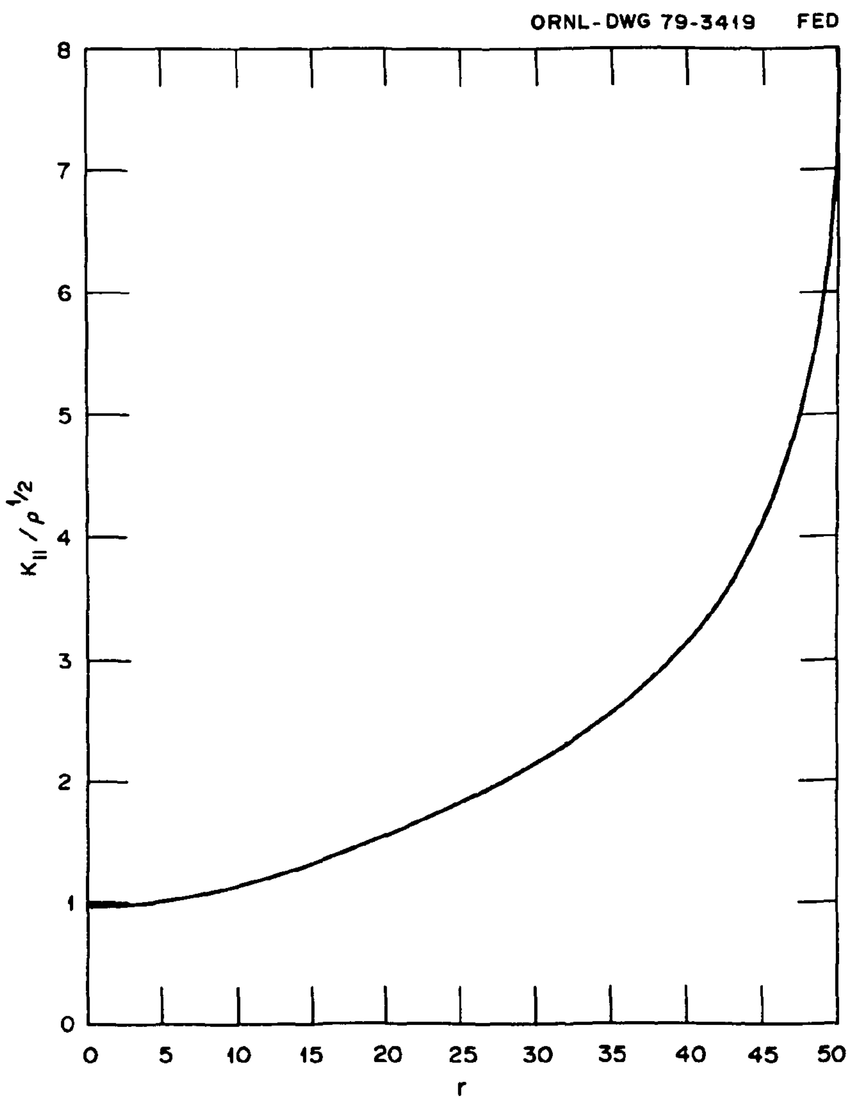

Fig. 1

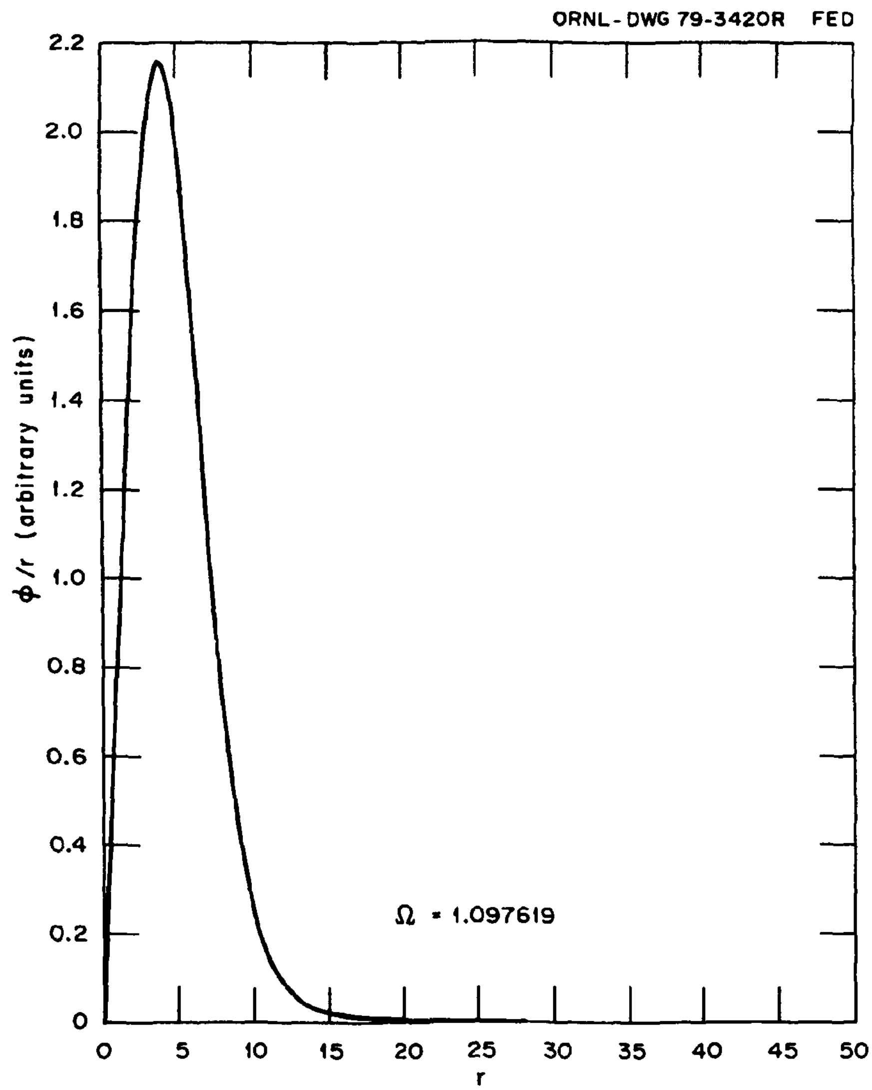
ORNL-DWG 79-3420R FED
2.2
2.0
1.8
1.6
1.4
1.2
1.0
0.8
0.6
0.4
0.2
0
ϕ/r (arbitrary units)
Ω = 1.097619
0
5
10
15
20
25
30
35
40
45
50
r

Fig. 2

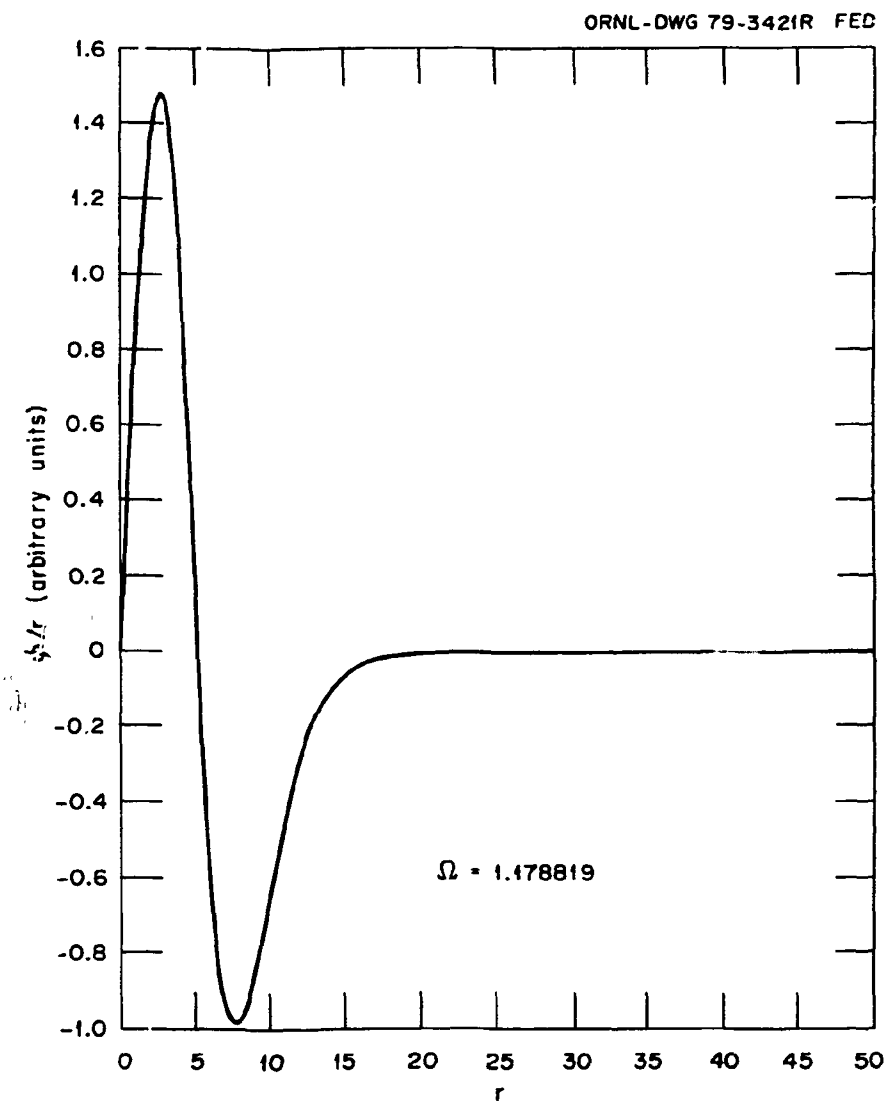
ORNL-DWG 79-3421R FED
1.6
1.4
1.2
1.0
0.8
0.6
0.4
0.2
0
-0.2
-0.4
-0.6
-0.8
-1.0
ψ/r (arbitrary units)
Ω = 1.178819
0
5
10
15
20
25
30
35
40
45
50
r

Fig. 3

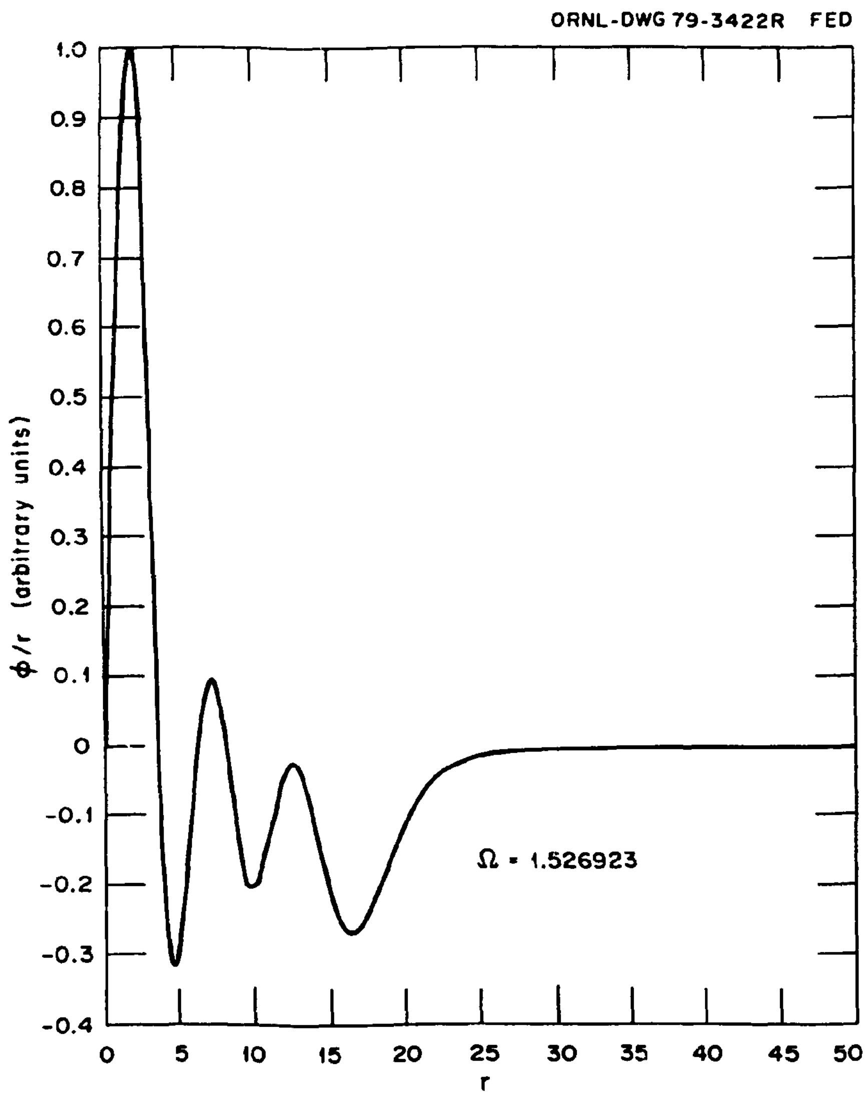
ORNL-DWG 79-3422R FED
1.0
0.9
0.8
0.7
0.6
0.5
0.4
0.3
0.2
0.1
0
-0.1
-0.2
-0.3
-0.4
φ/r (arbitrary units)
0
5
10
15
20
25
30
35
40
45
50
r
Ω = 1.526923

Fig. 4

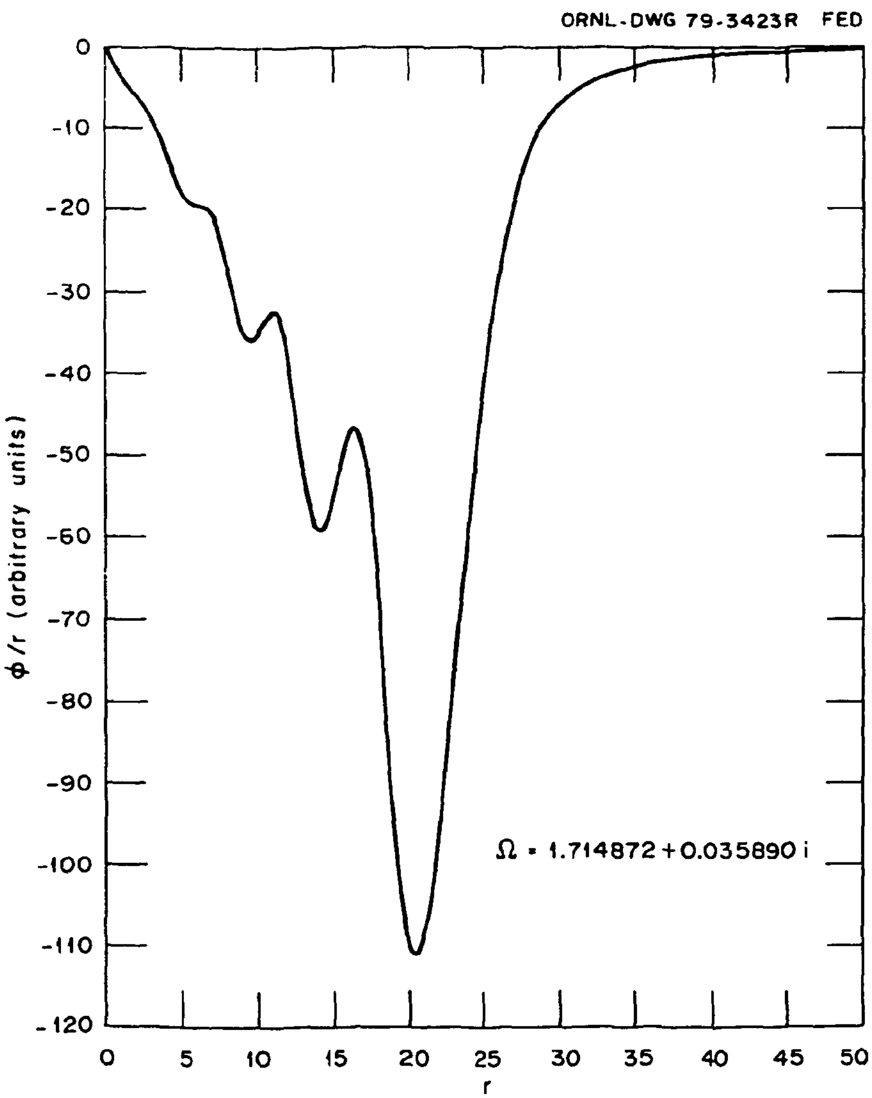
ORNL-DWG 79-3423R FED
0
-10
-20
-30
-40
-50
-60
-70
-80
-90
-100
-110
-120
φ/r (arbitrary units)
Ω = 1.714872+0.035890 i
0
5
10
15
20
25
30
35
40
45
50
r

Fig. 5

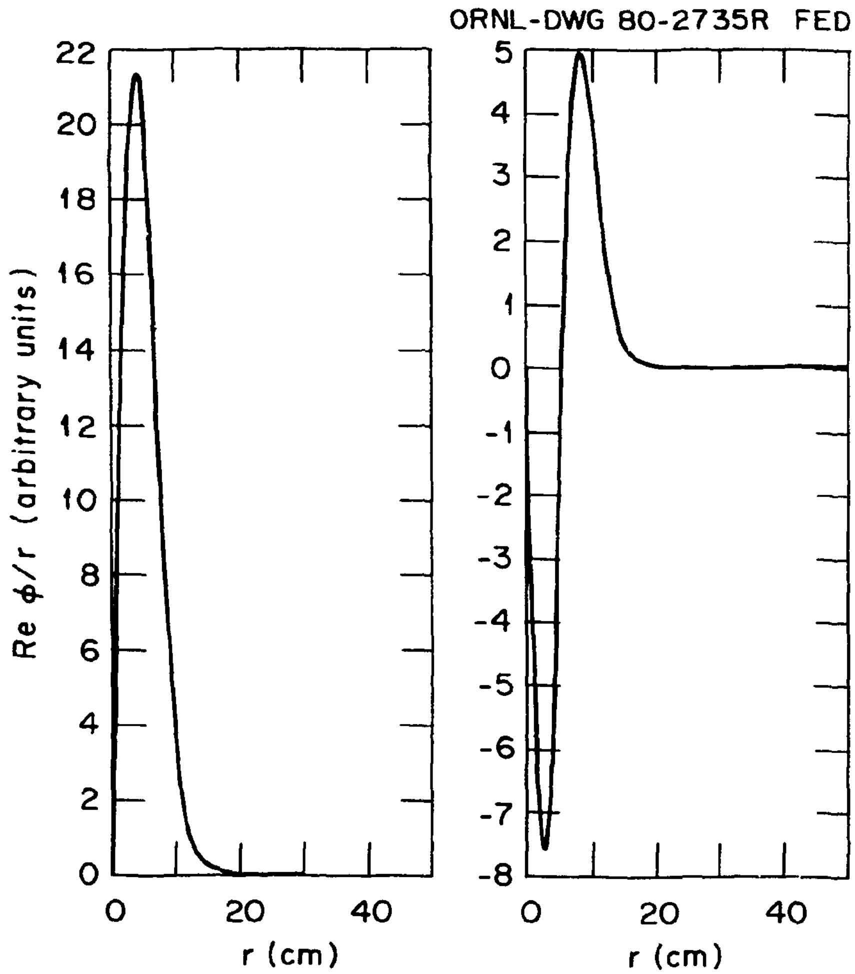
ORNL-DWG 80-2735R FED
Re ϕ/r (arbitrary units)
22
20
18
16
14
12
10
8
6
4
2
0
0
20
40
r (cm)
5
4
3
2
1
0
-1
-2
-3
-4
-5
-6
-7
-8
0
20
40
r (cm)

Fig. 6

ORNL-DWG 80-3243 FED

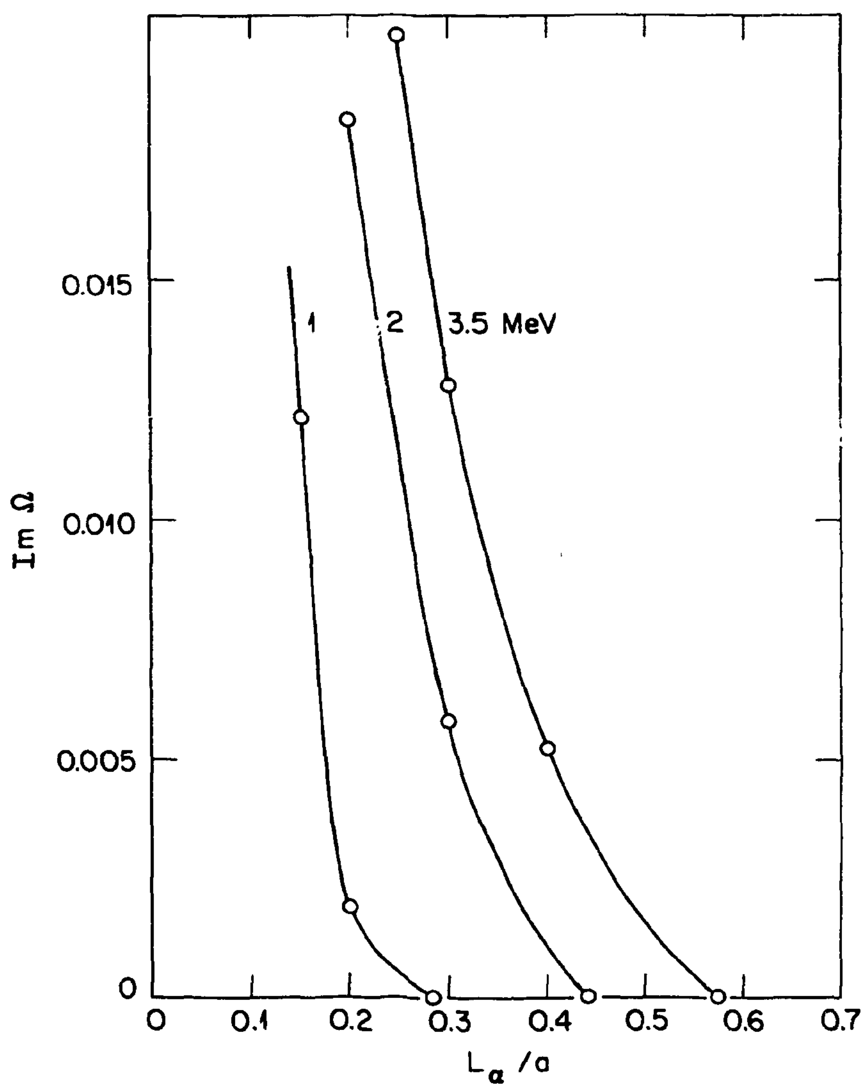

Fig. 7